Journal of Alloys and Compounds 509 (2011) 7434–7438

Contents lists available at ScienceDirect

Journal of Alloys and Compounds

journal homepage: www.elsevier.com/locate/jallcom

DC magnetization investigations in $Ti_{1-x}Mn_xO_2$ nanocrystalline powder

Sudesh Sharma [a], Sujeet Chaudhary [a,*], Subhash C. Kashyap [a], Vivek K. Malik [b]

[a] Department of Physics, Indian Institute of Technology Delhi, New Delhi 110016, India
[b] University of Fribourg, Department of Physics and Fribourg Center for Nanomaterials, Chemin du Musée 3, CH-1700 Fribourg, Switzerland

ARTICLE INFO

Article history:
Received 15 February 2011
Received in revised form 8 April 2011
Accepted 10 April 2011
Available online 20 April 2011

Keywords:
Dilute magnetic oxides
Titanium dioxide
Ferromagnetism
Defects

ABSTRACT

In the present paper, DC magnetization investigation on the insulating nanocrystalline powder samples of $Ti_{1-x}Mn_xO_2$ ($x = 0$, 0.05, 0.10, and 0.15) prepared by simple chemical route is reported. Structural measurements revealed phase pure anatase structure of TiO_2 when $x \leq 0.05$ and a mixture of anatase and rutile TiO_2 along with the signature of Mn_3O_4 phase for $x > 0.05$. Magnetic measurements exhibited the presence of ferromagnetic ordering at room temperature in samples having either small fraction of Mn or no Mn at all. This ferromagnetic signature is accompanied with paramagnetic contribution which is found to dominate with increase in Mn concentration. The $Ti_{1-x}Mn_xO_2$ sample having highest Mn concentration of $x = 0.15$ showed nearly paramagnetic behavior. However, at low temperatures, additional ferrimagnetic ordering arising due to Mn_3O_4 ($T_C = 42$ K) is evidenced in the doped samples. Consistent with the XRD investigations, the isofield DC-magnetization measurements under field cooled and zero field cooled (FC–ZFC) histories corroborated the presence of Mn_3O_4 phase. Also, distinct thermomagnetic irreversibility has been observed above 42 K. These results are suggestive of presence of weak ferromagnetic ordering possibly due to defects related with oxygen vacancies.

1. Introduction

Following the prediction of ferromagnetism in Mn doped GaAs [1], extensive research efforts have been started over dilute magnetic semiconductors (DMSs) to explore their possibility for application in spin based electronic devices [2]. Spin polarized carriers inducing exchange interaction between localized magnetic moments are found to be responsible for magnetic ordering in Mn doped GaAs DMSs [3]. For their practical use, a DMS should exhibit ferromagnetic Curie temperature (T_C) at/above room temperature. In starting stage, however, the electron density was confined only to 10^{19} cm^{-3}, and the hole doping in a semiconductor resulted in a T_C which was much less than room temperature [4,5]. Later, the transition metal (TM) doped oxide such as ZnO [6–10], SnO_2 [11–13], TiO_2 [14] emerged as appealing candidates, having T_C above room temperature, for their use in spin based electronic devices.

The research has extensively been focused on TM doped TiO_2 nanoparticles, thin films and single crystal for the last few years [15–19]. There are several reports available in the literature which report that the magnetic properties of Mn doped TiO_2 system are very sensitive to preparation method, morphology and post preparation treatment. It is reported that Mn doped TiO_2 film deposited by pulsed laser deposition (PLD) exhibited ferromagnetic (FM) ordering at room temperature and coupling between Mn magnetic moments via large concentration of holes might be responsible for the observed FM ordering [20]. On the other hand, Mn doping is assigned not to play any important role in introducing the ferromagnetism in TiO_2 thin films deposited by same technique (PLD) [21]. FM ordering at room temperature is reported in Mn doped TiO_2 thin films deposited by plasma assisted molecular beam epitaxy (PAMBE) and the observed FM is attributed to the formation of acceptor bound magnetic polarons [22]. Enhancement of RTFM due to higher concentration of oxygen vacancies was observed at low sintering temperature and in reduced atmosphere in bulk Mn doped TiO_2 powder samples, synthesized by solid state reaction method [23]. The magnetic behavior was found to be highly dependent on Mn concentration in Mn doped TiO_2 nanocrystals prepared by one-pot reaction under autogenic pressure at elevated temperature (RAPET) technique [17]. Coexistence of antiferromagnetic and ferromagnetic behavior was observed in Mn doped anatase TiO_2 nanowires prepared by hydrothermal method [24]. Mn doped TiO_2 nanoparticles were also found to be both superparamagnetic and paramagnetic at room temperature prepared by hydrothermal and sol–gel technique respectively [25,26]. These diverging inferences about the magnetic properties of the Mn doped TiO_2 system motivated us to further investigate the DC-magnetization behavior of nanoparticles of this system at different temperatures and under field cooled conditions.

* Corresponding author at: Thin Film Laboratory (TFL), Department of Physics, Indian Institute of Technology Delhi, Hauz Khas, New Delhi 110016, India.
Tel.: +91 11 26591341; fax: +91 11 26581114.
E-mail address: sujeetc@physics.iitd.ac.in (S. Chaudhary).

0925-8388/$ – see front matter © 2011 Elsevier B.V. All rights reserved.
doi:10.1016/j.jallcom.2011.04.072

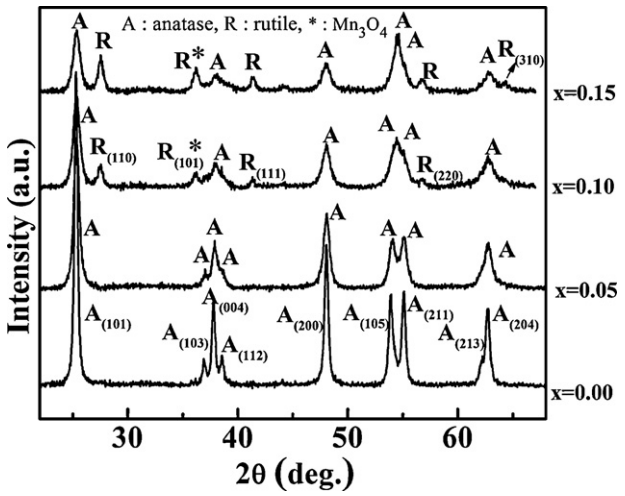

Fig. 1. X-ray diffractograms of $Ti_{1-x}Mn_xO_2$ nanopowders for $x = 0.00$, 0.05, 0.10 and 0.15.

2. Experimental details

Nanocrystalline powder samples of $Ti_{1-x}Mn_xO_2$ ($x = 0.00$, 0.05, 0.10 and 0.15) were prepared by chemical route. For the preparation of undoped TiO_2 powder, requisite amount of titanylacetylacetonate was first dissolved in ethanol and the solvent was then vaporized at ~80 °C with simultaneous rigorous stirring. The resulting gel-like product was then kept at 200 °C for 12 h. The lump thus obtained was ground and again heated in air at ~500 °C for 12 h in a box furnace. The as-prepared calcined powder was well ground and palletized. In a similar manner, nanopowders of Mn doped TiO_2 were also prepared by dissolving the requisite amount of manganese acetate tetrahydrate in addition to titanylacetylacetonate in ethanol. X-ray diffractometer with a goniometric resolution of 0.001° was employed to determine phases present in the nanopowder using Cu Kα radiation ($\lambda = 0.15406$ nm). A physical property measurement system (PPMS) from Quantum design QD6000 equipped with VSM P525 was used to record the field (H) and temperature (T) dependence of the magnetic moment of samples.

3. Results and discussion

The XRD patterns of $Ti_{1-x}Mn_xO_2$ ($x = 0.00$, 0.05, 0.10 and 0.15) powder samples recorded in Bragg–Brentano geometry of the diffractometer are shown in Fig. 1. These powder samples exhibit phase pure anatase structure of TiO_2 when $x \leq 0.05$ and a mixture of anatase and rutile TiO_2 for $x > 0.05$. No trace of either Mn clusters or any Ti/Mn binary oxides could be seen in any of the diffractograms within the detection limit of the instrument used. But the presence of most intense (2 1 1) Bragg's reflection from Mn_3O_4 phase (JCPDS card # 240734) is suspected around 2θ value of 36.1° at which the 2nd most intense diffraction peak due to (1 0 1) plane of rutile TiO_2 phase also appears (see Fig. 1). Crystallite size (t) of the observed TiO_2 phases is estimated by Sherrer's formula:

$$t = \frac{0.9\lambda}{(\beta_{h\,k\,l} - \beta^{s}_{h\,k\,l})\cos\theta_{h\,k\,l}} \quad (1)$$

where $\theta_{h\,k\,l}$ is the Bragg angle of the ($h\,k\,l$) reflection and λ is the wavelength of the X-ray used, $\beta^{s}_{h\,k\,l}$ is the full width at half maximum (FWHM) of standard silicon sample (used to correct the estimated size of crystallite for instrumental broadening) respectively.

The weight fraction of rutile phase present in the sample is estimated by using the empirical equation:

$$X_r = \frac{1}{1 + K(I_a/I_r)} \quad (2)$$

where I_a and I_r are the integrated peak intensities of the most intense anatase (1 0 1) and rutile (1 1 0) reflections and K is constant ~0.80 [27]. The values of crystallite size and weight fraction are shown in Table 1. Crystallite size of predominant anatase TiO_2 was found to decrease in the range 23–11 nm as the added Mn content is increased up to $x = 0.15$. Though the anatase to rutile (A–R) transformation is kinetically unfavorable at low temperature [28], evolution of rutile TiO_2 phase with increasing Mn content can be understood on the basis of changes in the activation energy involved. Activation energy is the required minimum energy for overcoming the energy barrier for A–R transformation. Smaller crystallite size of anatase TiO_2 (as observed in samples having higher Mn concentration) provides high surface to volume ratio, resulting in the increase in surface energy and hence the effective reduction in activation energy for the development of rutile phase of TiO_2. Once formed, the rutile grains consume the surrounding matrix of anatase and transform them synchronously [29].

Table 1
Calculated crystallite size (t) of anatase (A) and rutile (R) and wt.% of rutile in $Ti_{1-x}Mn_xO_2$ nanopowders.

Mn conc. 'x'	W_R (%)	t_A (nm)	t_R (nm)
0.00	–	23	–
0.05	–	15	–
0.10	22	12	42
0.15	41	11	37

We shall now argue that the XRD observations also indicate the finite incorporation of Mn ions at Ti^{4+} sites in TiO_2 matrix up to the maximum investigated value of Mn concentration 'x' = 0.15. It may be mentioned here that the radii of Mn-cations are very dependent on its oxidation state (Mn^{2+}: 0.82 Å, Mn^{3+}: 0.58 Å, Mn^{4+}: 0.53 Å) as compared to titanium (Ti^{4+}: 0.061 Å) for a coordination number of 6. Thus, the substitution of either Mn^{3+}/or Mn^{4+} at Ti^{4+} site in TiO_2 matrix is likely to result into the contraction of the lattice parameters. The incorporation of Mn^{3+}/or Mn^{4+} ions in TiO_2 at substitutional site in the present case is supported by the shifting of (1 0 5) XRD peak, as shown in Fig. 2, toward higher 2θ value on increasing Mn concentration. Both the lattice parameter 'c' and unit cell volume (V) were estimated and found to decrease from 9.507 to 9.409 Å and 136.055 to 134.795 $Å^3$, respectively as the

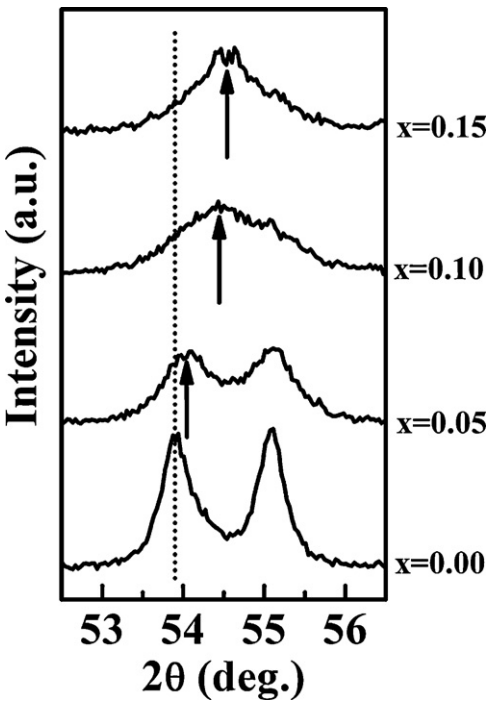

Fig. 2. Shift in (1 0 5) diffraction peak from anatase TiO_2 with the increase in Mn concentration 'x'. The arrow highlights the shift in peak position.

Table 2
Calculated lattice parameters and unit cell volume of $Ti_{1-x}Mn_xO_2$ nanopowders for anatase phase.

Mn conc. '*x*'	*a* (Å)	*c* (Å)	Unit cell volume (Å^3)
0.00	3.783	9.507	136.055
0.05	3.783	9.481	135.681
0.10	3.784	9.421	134.899
0.15	3.785	9.409	134.795

added concentration of Mn ('*x*') is increased from $x = 0$ to 0.15. Lattice parameter '*a*' was found practically unaltered with increase in Mn concentration. The data is summarized in Table 2. The observed small contraction in unit cell volume {maximum (0.8%) for Mn concentration $x = 0.15$} suggests that Mn^{3+}/or Mn^{4+} is most probable ionic form of Mn substituting in TiO_2 matrix. Thus, our XRD results suggest that incorporation of Mn in TiO_2 lattice did not reach to its solid solubility limit up to 15 at.% due to the observed shifting of XRD peaks toward higher 2θ values even in $x = 0.15$ case. As mentioned above, absence or presence of Mn_3O_4 as an impurity phase cannot be clearly ascertained from the XRD investigations. Moreover, the calculation of intensity ratio of (1 0 5) and (1 0 1) anatase peaks shows a systematic increase from 0.27 to 0.84 on increasing Mn concentration (see Fig. 3). This is understandable as the substitution of manganese in TiO_2 lattice is expected to affect the structure factor of TiO_2 lattice, and hence the intensity of diffraction peaks. Recently, we have shown systematic evolution of XRD peaks in Co doped TiO_2 films due to the substitution of Co in TiO_2 lattice [30].

For the investigation of magnetic properties of the samples, analysis of isothermal magnetization curves recorded at room (300 K) and low (10 K, 38 K) temperatures using PPMS has been carried out. Fig. 4(a) shows the variation of as-observed magnetization (*M*) with magnetic field (*H*) recorded at room temperature for undoped and doped powders. Except in the case of sample having $x = 0.15$, the presence of low field nonlinear variation of *M* with *H*, suggests the presence of a ferromagnetic phase in all the samples. The linear contribution, which can originate from either a paramagnetic (PM) or an antiferromagnetic (AF) or a diamagnetic (DM) phase, is clearly Mn-concentration dependent in these $Ti_{1-x}Mn_xO_2$ samples. It may be noted that observed *M*–*H* behavior of the pure TiO_2 is a result of mixed contributions arising most probably due to the expected diamagnetic TiO_2 and additional weak ferromagnetic phase. The change of slope of the *M*–*H* curve (in high field region) suggests the presence of more than one phases in the sample that follow linear *M*–*H* variation (PM and AF or two paramagnetic phases, etc.). At Mn conc. $x = 0.15$, the sample exhibited paramagnetic like behavior at room temperature. It may be noted that as the Mn concentration is increased, the slope of the high field paramagnetic like linear *M*–*H* behavior of the samples gets affected. This shows the utilization of added Mn in different phases having different susceptibilities. We are of the view that this change in the slope on increasing Mn concentration '*x*' cannot be attributed entirely due to increase in number of non-interacting (PM) Mn-spins.

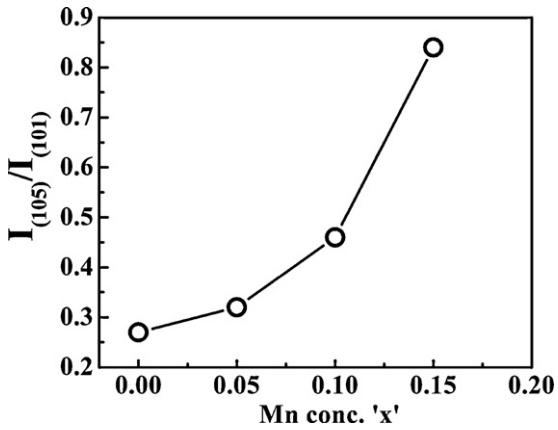

Fig. 3. Variation in intensity-ratio of (1 0 5) and (1 0 1) Bragg's reflections of anatase $Ti_{1-x}Mn_xO_2$ nanopowders with increase in Mn concentration '*x*'.

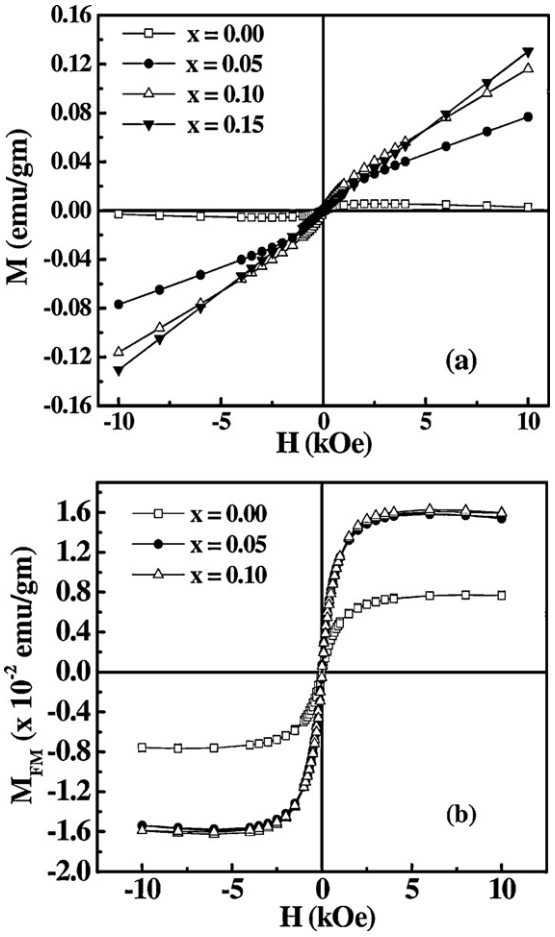

Fig. 4. *M*–*H* curves of $Ti_{1-x}Mn_xO_2$ nanopowders, (a) as-recorded data for $x = 0.00$, 0.05, 0.10 and 0.15 at 300 K, and (b) extracted *M*–*H* behavior of FM fraction for $x = 0.00$, 0.05 and 0.10 at 300 K.

The *M*–*H* behavior of the FM fraction, extracted from data of Fig. 4(a), is shown in Fig. 4(b). As can be seen form the figure, that the value of the saturation magnetization (M_s) in 5 and 10 at.% Mn substituted samples does not depend on Mn concentration and lie around 1.62×10^{-2} emu/g. Quite remarkably, at $x = 0.15$, the FM contribution practically disappears. Lowering of magnetization with increase in the concentration of Cu in CeO_2 has also been reported [31]. None of the oxide phases of Mn, including Ti/Mn oxides (such as $MnTiO_3$, Mn_2Ti_4O and $MnTi_2O_4$), could be responsible for observed ferromagnetic behavior at room temperature even if it is present in our samples, as none of these manganese oxides is ferromagnetic at room temperature. Moreover, ferrimagnetic Mn_3O_4 has Curie temperature $T_C = 42$ K [32] which is too low to account for the observed RTFM.

For gaining further insight, the *M* vs. *T* (ZFC–FC) scans were also recorded in addition at 1000 Oe magnetic field by varying the temperature down to 10 K. We present in Fig. 5(a), (b) and (c), the *M* vs. *T* (ZFC–FC) plots for Mn incorporated powder samples with $x = 0.05$, 0.10 and 0.15 respectively, recorded in the presence of 1000 Oe applied magnetic field. Observation of small kink around 42 K {see insets of Fig. 5(a)–(c)} in M^{ZFC}–*T* curve and shoulder in

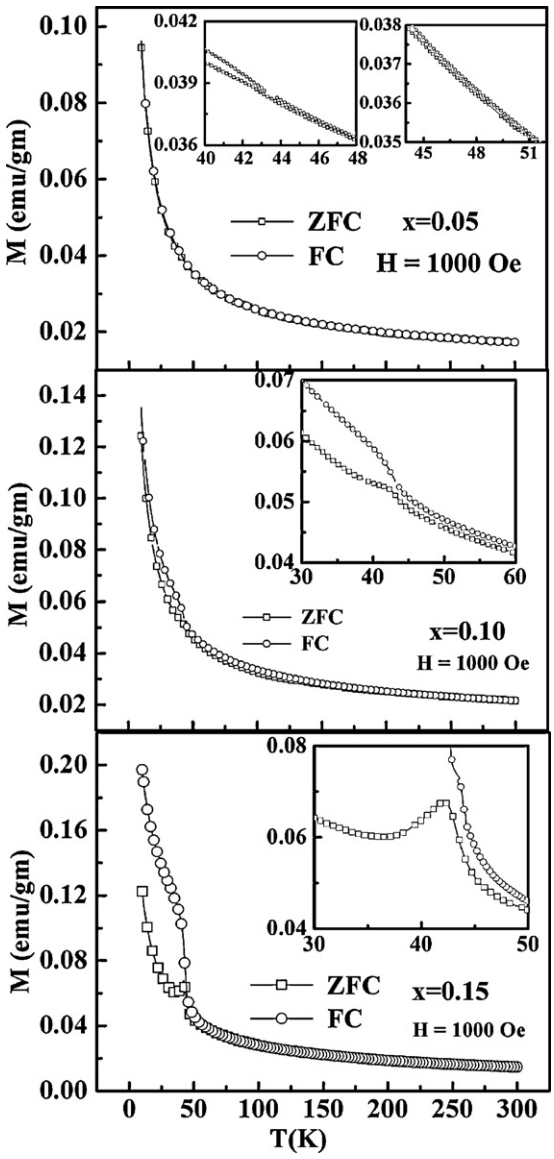

Fig. 5. M vs. T (ZFC–FC) data of $Ti_{1-x}Mn_xO_2$ nanopowders for (a) $x = 0.05$, (b) $x = 0.10$ and (c) $x = 0.15$. Inset in each figure shows the presence of kink around 42 K. Presence of TMI even above 42 K is particularly notable.

M^{FC}–T curve is understandably due to the presence of ferrimagnetic Mn_3O_4. Together with the XRD findings, this feature now clearly proves the presence of Mn_3O_4 in all the three doped samples. Furthermore, it can be clearly seen from the main panel in Fig. 5(a)–(c) and the insets therein that as the concentration of Mn is increased the kink and shoulder become more and more prominent due to the increased volume fraction of ferrimagnetic Mn_3O_4, with the result that highest thermomagnetic irreversibility (TMI) i.e., $M^{FC}(T) \neq M^{ZFC}(T)$, is observed in samples having highest Mn concentration. These results clearly show that incorporation of Mn in TiO_2 is partial and increase of Mn-concentration results in more and more formation of Mn_3O_4, which at room temperature, will also contribute to PM like magnetization behavior, in addition to the PM coming from Mn-ions substituted in TiO_2 lattice. In our opinion, relatively higher amount of Mn_3O_4 in 15 at.% Mn doped powder sample could be responsible for the predominant PM like behavior seen in its overall M–H plot recorded at RT.

In the low temperature region, distinctly sharp rise in moment can be seen in both the field cooled magnetization as well as zero field cooled magnetization M–T curves for all the samples.

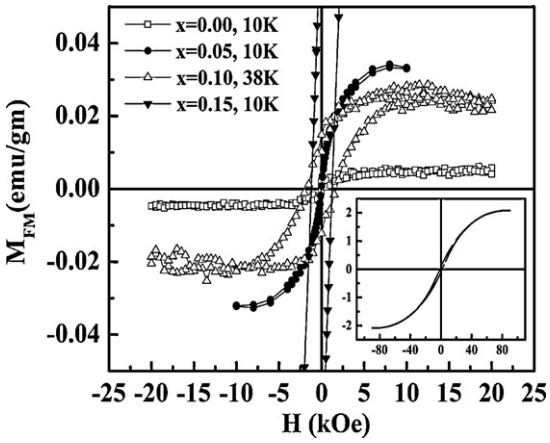

Fig. 6. Extracted M–H behavior of FM fraction of $Ti_{1-x}Mn_xO_2$ nanopowders for $x = 0.00$, 0.05, and 0.10 at indicated low temperatures. Inset shows the complete extracted M–H loop for $x = 0.15$ sample at 10 K.

This sharp rise of M at low temperatures, which is typical of PM-like magnetization behavior, is additional signature of Mn-incorporation in TiO_2 lattice. The observation of substantial TMI even in relatively high applied magnetic field strength of 1000 Oe suggests the definite presence of FM ordering, although it is weak in strength. Thus, on the basis of XRD and magnetic measurements one can conclude that added Mn is incorporated in TiO_2 in two different ways: (i) some of Mn ions substitute Ti^{4+} sites in the TiO_2 lattice, and (ii) some Mn-ions form separate phase of manganese oxide (Mn_3O_4), possibly due to the either limited solubility of Mn in TiO_2 lattice or lower energy of formation of Mn_3O_4. Thus, Mn doped TiO_2 powder heated at 500 °C, in the present case, is a mixture of different phases: paramagnetic $Ti_{1-x}Mn_xO_2$ (due to the substitutional Mn ions) and Mn_3O_4 (ferrimagnetic below 42 K, and paramagnetic above 42 K). However, to account for observed FM behavior at RT, additional mechanism of magnetic ordering needs to be identified which can explain the observed ferromagnetic contribution at RT.

We now present and discuss the low temperature M–H behavior of these samples. The M–H loops have been recorded on both the doped and undoped samples. At low temperatures (10–38 K), all these samples exhibited magnetization M–H behavior identical to that observed at RT by $Ti_{1-x}Mn_xO_2$ sample (up to $x = 0.10$). The extracted FM fraction for all the samples is shown in Fig. 6. The value of saturation magnetization at room temperature is observed to increase from a value of ~0.016 emu/g to 0.034 and 0.026 emu/g for 5 and 10 at.% Mn doped sample respectively. It is remarkable that a clear hysteresis is observed for 15 at.% Mn doped TiO_2 sample at 10 K, though at room temperature, this sample exhibited linear M–H behavior. Since the samples having Mn concentration up to 10 at.% have shown non-linear M–H behavior even at room temperature, the observed M–H loop at low temperature (<42 K) cannot be entirely governed by ferrimagnetic Mn_3O_4 ($T_C \sim 42$ K) impurity phase. This conjecture is also supported by the presence of clear TMI, as can be seen in inset of Fig. 5(a)–(c), well above the T_C of ferrimagnetic Mn_3O_4 impurity phase. One possible contribution to this ferromagnetic behavior can result from the FM coupling between defect states in these samples at room temperature, as proposed previously in a few reports [33,34]. Thus, at low temperature, the overall magnetic behavior of these samples might correspond to a mixture of both ferromagnetic coupling between defect states present in the samples and ferrimagnetic contribution coming from Mn_3O_4 phase below 42 K.

The weak FM character ($M_s \sim 0.007$ emu/g) observed at RT in the magnetization behavior of the pure TiO_2 could result from oxygen vacancies or defects which are quite likely to be formed

in the oxides. There exists similar reports wherein FM ordering is ascribed to oxygen defects in samples of pure TiO_2 [33], ZnO [34], etc. Recently, Wen et al. [35] have reported small magnetization of 0.004 emu/g. This value is quite comparable to that observed in our undoped sample, after grinding into fine powder. Further, the carrier mediated exchange interaction such as Rudermunn–Kittel–Kasuya–Yoshida (RKKY) could not be responsible for the observed relatively stronger saturation magnetization in 5 and 10 at.% Mn incorporated TiO_2 samples due to their highly resistive nature. The model based on the formation of bound magnetic polarons (BMPs) [36,37], which are expected to be formed in insulating samples (which is actually the case in present $Ti_{1-x}Mn_xO_2$ samples having resistivity $\rho \sim 10^7$ Ω-m) may account for the observed RTFM in these doped samples containing relatively large number of magnetic spins (in comparison to numbers of carriers present), such as in the present case. However, nearly non-existent FM in 15 at.% Mn incorporated TiO_2 powder hints some kind of compensation taking place from the additional AF fluctuations, as more and more Mn is added to TiO_2 lattice. The limited sensitivity of PPMS (as opposed to that in SQUID) precluded the observation of relatively weak FM signal in 15 at.% Mn incorporated TiO_2 powder. Additional microscopic and local as well as element specific magnetization investigations, such as XMCD are needed to actually ascertain and understand the cause of the ferromagnetic ordering in $Ti_{1-x}MnO_2$ powder samples. We also note that the lower values of magnetization at room temperature suggest that Mn-doped TiO_2 system is not worthy for practical applications for futuristic spintronic devices.

4. Conclusions

Room temperature ferromagnetic (FM) ordering is reported in insulating nanocrystalline powder samples of $Ti_{1-x}Mn_xO_2$ prepared by simple chemical route. Magnetization and structural investigations revealed the simultaneous formation of Mn_3O_4 phase and partial substitution of Mn ions in TiO_2 lattice up to the highest investigated Mn concentration of 15 at.%. Both the undoped and doped (except 15 at.% Mn incorporated TiO_2 powder) samples exhibited non-linear magnetization behavior at room temperature. Saturation magnetization in doped samples was found to be independent of added Mn concentration. Low temperature *M–T* measurements of doped sample suggest the presence of weak FM ordering in all the samples. Formation of oxygen vacancies/defects and bound magnetic polarons (in which both the oxygen vacancy and magnetic ions are involved) are proposed to be responsible for observed FM ordering in undoped and doped samples, respectively.

Acknowledgements

The authors thankfully acknowledge Dr. V.P.S. Awana and Mr. Anuj (National Physical Laboratory, India) and Ms. Aakanksha Sehgal (IIT Roorkee, India) for magnetic measurements. One of the authors (S.S.) would like to thank the University Grant Commission (UGC) for providing the Senior Research Fellowship.

References

[1] T. Dietl, H. Ohno, F. Matsukur, J. Cibert, D. Ferrad, Science 287 (2000) 1019.
[2] I. Zutic, J. Fabian, S.D. Sarma, Rev. Mod. Phys. 76 (2004) 323.
[3] F. Matsukura, H. Ohno, A. Shen, Y. Sugawara, Phys. Rev. B 57 (1998) R2037.
[4] T. Fukumura, H. Toyosaki, Y. Yamada, Semicond. Sci. Technol. 20 (2005) S103.
[5] H. Ohno, A. Shen, F. Matsukura, A. Oiwa, A. Endo, S. Katsumoto, Y. Iyc, Appl. Phys. Lett. 69 (1996) 363.
[6] Z.L. Lu, W. Miao, W.Q. Zou, M.X. Xu, F.M. Zhang, J. Alloys Compd. 494 (2010) 392.
[7] M. Snure, D. Kumar, A. Tiwari, Appl. Phys. Lett. 94 (2009) 012510.
[8] K.P. Bhatti, S. Chaudhary, D.K. Pandya, S.C. Kashyap, J. Appl. Phys. 101 (2007) 103919.
[9] M. Snure, A. Tiwari, J. Appl. Phys. 106 (2009) 043904.
[10] K.P. Bhatti, S. Chaudhary, D.K. Pandya, S.C. Kashyap, J. Appl. Phys. 101 (2007) 033902.
[11] J.M.D. Coey, A.P. Douvalis, C.B. Fitzgerald, M. Venkatesan, Appl. Phys. Lett. 84 (2004) 1332.
[12] K. Gopinadhan, S.C. Kashyap, D.K. Pandya, S. Chaudhary, J. Appl. Phys. 102 (2007) 113513.
[13] S.C. Kashyap, K. Gopinadhan, D.K. Pandya, S. Chaudhary, J. Magn. Magn. Mater. 321 (2009) 957.
[14] Y. Matsumoto, M. Murakami, T. Shono, T. Hasegawa, T. Fukumura, M. Kawasaki, P. Ahmet, T. Chikyow, S. Koshihara, H. Koinuma, Science 291 (2001) 854.
[15] K. Yamaki, N. Shimizu, E. Kita, T. Mochiku, H. Fujii, K. Yamada, S. Itoh, K. Kadowaki, Phys. Stat. Sol. C 3 (2006) 4127.
[16] L. Sangaletti, M.C. Mozzati, P. Galinetto, C.B. Azzoni, A. Speghini, M. Bettinelli, G. Calestani, J. Phys.: Condens. Matter 18 (2006) 7643.
[17] S. Bhattacharyya, A. Pucci, D. Zitoun, A. Gedanken, Nanotechnology 19 (2008) 495711.
[18] L.F. Liu, J.F. Kang, Y. Wang, H. Tang, L.G. Kong, L. Sun, X. Zhang, R.Q. Han, J. Magn. Magn. Mater. 308 (2007) 85.
[19] R.K. Singhal, A. Samariya, Y.T. Sudhish Kumar, D.C. Xing, S.N. Jain, U.P. Dolia, T. Deshpande, E.B. Shripathi, Saitovitch, J. Appl. Phys. 107 (2010) 113916.
[20] Z. Wang, J. Tang, Y. Chen, L. Spinu, W. Zhou, L.D. Tung, J. Appl. Phys. 95 (2004) 7384.
[21] N.H. Hong, J. Sakai, A. Ruyter, V. Brize, Appl. Phys. Lett. 89 (2006) 252504.
[22] X. Li, S. Wu, P. Hu, X. Xing, Y. Liu, Y. Yu, M. Yang, J. Lu, S. Li, W. Liu, J. Appl. Phys. 106 (2009) 043913.
[23] Z.M. Tian, S.L. Yuan, J.H. He, Y.Q. Wang, P. Li, H.Y. Xie, L. Liu, S.Y. Yin, Solid State Commun. 142 (2007) 545.
[24] L.H. Mie, L. Min, Z.Y. Su, H.T. Cheng, J. Cent. South Univ. Technol. 17 (2010) 239.
[25] Z.V. Saponjic, N.M. Dimitrijevic, O.G. Poluektov, L.X. Chen, E. Wasinger, U. Welp, D.M. Tiede, X.B. Zuo, T. Rajh, J. Phys. Chem. B 110 (2006) 25441.
[26] G. Glaspell, A. Manivannan, J. Cluster Sci. 16 (2005) 501.
[27] R. Spurr, H. Myers, Anal. Chem. 29 (1957) 760.
[28] K. Nair, P. Kumar, Scr. Metall. Mater. 32 (1995) 873.
[29] P.I. Gauma, P.K. Dutta, M.J. Mills, Nanostruct. Mater. 11 (1999) 1231.
[30] S. Sharma, S. Chaudhary, S.C. Kashyap, J. Phys. D: Appl. Phys. 43 (2010) 015007.
[31] P. Slusser, D. Kumar, A. Tiwari, Appl. Phys. Lett. 96 (2010) 142506.
[32] K. Dwight, N. Menyuk, Phys. Rev. 119 (1960) 1470.
[33] D. Kim, J. Hong, Y.R. Park, K.J. Kim, J. Phys.: Condens. Matter 21 (2009) 195405.
[34] M. Kapilashrami, J. Xu, V. Ström, K.V. Rao, L. Belova, Appl. Phys. Lett. 95 (2009) 033104.
[35] Q.Y. Wen, H.W. Zhang, Y.Q. Song, Q.H. Yang, H. Zhu, J.Q. Xiao, J. Phys.: Condens. Matter 19 (2007) 246205.
[36] A. Kaminski, S.D. Sarma, Phys. Rev. Lett. 88 (2002) 247202.
[37] J.M.D. Coey, M. Venkateshan, C.B. Fitzgerald, Nat. Mater. 4 (2005) 173.